

Pathogen Induced Tolerance

Sean P. Stromberg* and Jean Carlson†

Physics Department

University of California Santa Barbara

(Dated: May 15, 2008)

Abstract

Using a dynamic model we study the adaptive immune response to a sequence of two infections. As expected, memory cells generated by the first (primary) infection generate rapid response when the secondary infection is identical (homologous). When the secondary infection is different (heterologous), the memory cells have a positive effect or no effect at all. In exceptional instances in nature the primary infection generates vulnerability to a heterologous infection. This model predicts “Original Antigenic Sin”, but shows that average effector affinity is not an accurate measure of the quality of an immune response, and does not on its own provide a mechanism for vulnerability. In this paper we propose and mathematically study a novel mechanism “Pathogen Induced Tolerance” (PIT), where antigen from the primary infection takes part in the immune system tolerance mechanisms, prohibiting the creation of new naive cells specific for the secondary response. The action of this mechanism coincides with Original Antigenic Sin but is not caused by it. We discuss the model in the context of the dengue virus and show that PIT is better suited to describe observed phenomena than the proposed Antibody Dependant Enhancement (ADE).

*Electronic address: stromberg@physics.ucsb.edu

†Electronic address: carlson@physics.ucsb.edu

I. INTRODUCTION

The response of the adaptive immune system of vertebrates [1] is a function of past infectious disease exposures. An immune response can have several different effects on future exposures: immunity for identical or nearly identical diseases, some amount of cross-reactive protection for similar diseases, no effect for unrelated diseases, and in exceptional cases an increased vulnerability.

The adaptive immune system derives the ability to respond to new infections from a diverse population of naive cells each one having a unique and randomly selected set of chemicals to which it responds [2–4]. This randomness produces a large number of cells that would respond to non-pathogenic native and environmental chemicals. These autoreactive and allergenic naive cells are eliminated before they reach maturity. Once mature, a naive cell that comes into contact with a chemical it recognizes is triggered to proliferate and generate an immune response eliminating that chemical and leaving behind a large clone of long-lived memory lymphocytes. These memory cells provide future immunity to subsequent infections with the same chemical markers.

The adaptive immune system is composed of B and T white blood cells (i.e. lymphocytes). These cell types derive their self, non-self discrimination ability from the binding specificity of their receptors: T cell receptors for T cells, and membrane bound antibody for B cells. These receptors are assembled randomly from gene segments (VDJ recombination), producing a population of pre-naive cells, in which each individual combination has a different binding specificity. This population having randomly arranged receptors contains a large fraction of cells which bind to the body's own chemicals. These autoreactive pre-naive cells are triggered to die by apoptosis when they recognize antigen (Negative Selection). The pre-naive cells that are not triggered to die, mature to become short-lived naive cells. This diverse population, having receptors composed of random combinations of genes, gives the immune system the ability to respond to many pathogens.

During an infection antigen is introduced to the immune system. The cells whose receptors recognize the antigen proliferate (Positive Selection) and differentiate within the lymph nodes into antigen removing effector cells and long-lived memory cells. The memory cells provide an increased defense to future infections giving rise to more rapid and efficient responses for identical secondary infections (immunity).

In addition to immunity for a homologous secondary infection, the memory cells left after an immune response will have either a positive effect or no effect at all on a heterologous secondary infection depending on how strongly they bind to the new antigen. There are numerous examples of diseases that have such a cross-reactivity for each other [5] including cowpox and smallpox, influenza A and hepatitis C, rotavirus and HIV-1, and choriomeningitis virus and pichinde virus. In some disease systems a negative effect on heterologous immune responses has been observed [6, 7].

In this paper we use a dynamical model of the adaptive immune response [8] to study the effects of cross-reactivity in a pair of infections (termed primary and secondary). This model uses differential equations to model the behavior of antigen proliferation, lymphocyte stimulation, antigen removal by effector lymphocytes, and effector death. Our model includes the dynamics of the diverse population of lymphocytes which we organize using generalized shape space models [9]. We introduced and studied the model previously in the context of immunosenescence focusing on long term consequences of the natural adaptive mechanism [8].

We first consider immunity for homologous secondary infections. We then consider cross-reactive memory cells for heterologous secondary infections. We compare a range of secondary antigens with differing degrees of similarity to the primary antigen and observe the effect of “Original Antigenic Sin” where effectors for the primary infection dominate the secondary response [10, 11]. We also see that as the antigenic difference increases, so does the severity of the infection. Under no conditions in the basic model do we see the severity increase beyond that for the primary infection, even for cases with antigenic sin.

To explain situations where increased severity to heterologous infections is observed, we present and study a novel mechanism “Pathogen Induced Tolerance,” (PIT). In this mechanism the antigens from a primary infection also participate in negative selection. When this occurs, the primary infection initially provides cross-reactive protection that decays over a period of months to an increased severity for a range of secondary antigen similarities. The lack of high affinity naive cells specific for the heterologous secondary infection generates the increased severity. It has been hypothesized that primary and secondary infections with different serotypes of the dengue virus produces more severe symptoms [6, 12]. We compare the model with observations for the dengue virus, and contrast PIT with other proposed mechanisms such as “Antibody Dependant Enhancement.”

II. RESULTS

A. Immune Response Model

The model used in this paper was initially introduced and studied in the context of long term effects on the lymphocyte repertoire due to memory cell accumulation over a sequence of 400 unrelated infections [8]. In this study we look at the effects of a sequence of two infections that have a chemical similarity.

In the previous study there were many different distinct diseases that could infect the system one at a time. The diseases were sufficiently different that there was no cross-reactive protection conferred by previously accumulated memory cells. The previous study included dynamics for the trapping and presentation of antigen by dendritic cells, long term regulation of lymphocyte number, and the relaxation to the equilibrium state between infections. In the previous study we derived an approximation from the full model by assuming the amount of antigen presented by dendritic cells is constant during the immune response. This approximation neglects the process of antigen trapping and is only accurate during the immune response. The approximation enables analytic solution.

In this paper we use the approximate form of the model, as its reduced complexity is adequate for the dynamics we are interested in here. We ignore the long term homeostatic effects discussed in the previous paper as they are relevant for memory accumulation over a lifetime. Here we are interested in a sequence of two infections having some degree of cross-reactivity.

The reactions considered in this paper are shown diagrammatically in Fig. 1 and the cell types are described in Table I. From the left: pre-naive cells P can be stimulated by antigen presented on dendritic cells (H) to apoptose. This negative selection reaction acts to remove autoreactive cells. If a pre-naive cell survives negative selection it will mature to a naive cell (N). Naive cells can be stimulated in the same way by H but proliferate into memory (M) and effector cells (E). Naive cells that do not bind antigen die by apoptosis. The naive population is replaced with new naive cells every few months [13]. Memory cells are long-lived but otherwise identical in our model to naive cells. The memory cells can be stimulated in the same manner as naive cells, proliferating into more memory cells and effector cells. The effector cells are short-lived and do the work of removing the antigen (A)

from the body. Antigen growth via reproduction of the associated pathogen is also shown on the far right.

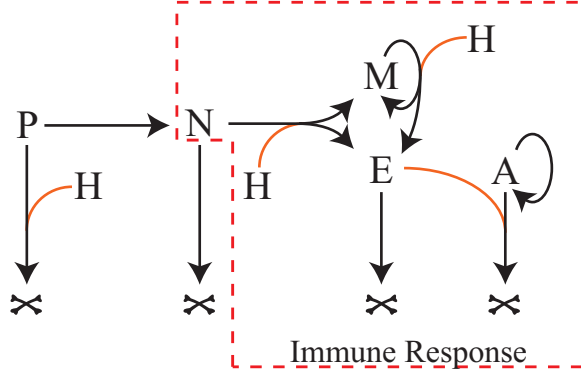


FIG. 1: This flowchart summarizes the reactions considered in our model. The leftmost reaction shows pre-naive cells (P) subjected to negative selection. Those pre-naive cells that survive negative selection become short-lived, continuously recycled naive cells (N). The red box surrounds reactions taking place during an immune response and modeled with differential equations. The reactions shown in orange are affinity dependent.

As the reactions considered here are common to both T-cells and B-Cells, we do not make a distinction between them in our model. This technique has been used in past generalizations [4]. Additionally, we do not consider many immune system effects such as T-help, somatic hypermutation [10], or the complexities of germinal center reactions [14, 15], which we do not consider to be limiting in the phenomena considered here.

1. Shape Space

In order to model an immune response with large diversity of lymphocytes we use the generalized shape space technique of Oster and Perelson [9], where the binding characteristics of a lymphocyte receptor and an antigen are described by vectors in a high dimensional space. The various dimensions of the space correspond not only to the geometry of the binding site but also the relative parameters such as electro-negativity and hydrophobicity. For a Euclidian metric such as what is used in this paper, this high dimensional space has been estimated to be between five and eight dimensions [16]. In this paper we use two dimensions for illustrative purposes and consider a very small region of the total shape space

Species	Symbol	Primary Function
Pre-Naive	$P(\vec{y}, t)$	Immature lymphocytes generated in the bone marrow with randomly assembled receptors. If stimulated with presented antigen $H(\vec{x})$ they die by apoptosis. Otherwise they mature into naive cells.
Antigen	$A(\vec{x}, t)$	Chemical that stimulates an immune response, which acts to remove it from the body.
Presented Antigen	$H(\vec{x})$	Antigen $A(\vec{x}, t)$ that has been captured by dendritic cells and is presented to lymphocytes. This quantity is approximately constant during an immune response. The dynamics of antigen capture and the constant approximation are discussed in the context of this model in [8].
Effector	$E(\vec{y}, t)$	Short-lived cells that remove antigen from the body.
Naive	$N(\vec{y}, t)$	Short-lived lymphocytes. If stimulated these will divide into memory and effector cells.
Memory	$M(\vec{y}, t)$	Long-lived lymphocytes that, like naive cells, when stimulated divide into more memory and effector cells.

TABLE I: Cell types in the model. The dynamics of these populations are pictorially represented in Fig. 1 and dynamic equations are given in Eq. 2-5. All populations have binding characteristics represented as vectors in an abstract shape space. Increasing proximity between antigen vector \vec{x} and effector receptor vector \vec{y} corresponds to increasing efficacy of that cell population's response.

in the neighborhood of the antigen vector for the primary infection.

If an antigen's binding vector \vec{y} and a receptor's binding vector \vec{x} are equal, the affinity $\gamma(\vec{x}, \vec{y})$ is maximal: $\gamma(\vec{x}, \vec{y}) = \gamma_m$. If $\vec{x} \neq \vec{y}$, $\gamma(\vec{x}, \vec{y})$ is a decaying function of the Euclidian distance in the shape space. As in Segel and Perelson [4], we take the affinity vs. distance relation to be a Gaussian:

$$\gamma(\vec{x}, \vec{y}) = \gamma_m e^{-(\vec{x}-\vec{y})^2/2b^2}, \quad (1)$$

The term b sets the scale for the shape space and is a measure of the specificity of antigen recognition in the shape space.

2. Dynamic Equations

The antigen and lymphocyte populations correspond to densities on the shape space. The presented antigen $H(\vec{x})$ which is trapped and presented on the surface of dendritic cells, preserves the shape space vector of the original antigen $A(\vec{x}, t)$. The dynamic model of cell populations during an immune response is derived as an approximation from a larger model, as is discussed in depth in [8]. The reactions enclosed in the red box of Fig. 1 are fast rate reactions, taking place during an immune response. The dynamics are modeled with a system of differential equations:

$$\frac{\partial A(\vec{x}, t)}{\partial t} = \beta A(\vec{x}, t) - A(\vec{x}, t) \int \gamma(\vec{x}, \vec{y}) E(\vec{y}, t) d\vec{y}; \quad (2)$$

$$\frac{\partial E(\vec{y}, t)}{\partial t} = 2f\alpha H(\vec{x})\gamma(\vec{x}, \vec{y})[N(\vec{y}, t) + M(\vec{y}, t)] - \delta E(\vec{y}, t); \quad (3)$$

$$\frac{\partial N(\vec{y}, t)}{\partial t} = -\alpha H(\vec{x})\gamma(\vec{x}, \vec{y})N(\vec{y}, t); \quad (4)$$

$$\frac{\partial M(\vec{y}, t)}{\partial t} = (2 - 2f)\alpha H(\vec{x})\gamma(\vec{x}, \vec{y})N(\vec{y}, t) + (1 - 2f)\alpha H(\vec{x})\gamma(\vec{x}, \vec{y})M(\vec{y}, t). \quad (5)$$

The populations described here are the same as described in Table I above and found in Fig. 1.

The antigen $A(\vec{x}, t)$, is associated with pathogen and is modeled in these equations as growing exponentially in the absence of an immune response. The naive cells $N(\vec{y}, t)$, are short-lived lymphocytes that can be stimulated by antigen to proliferate into memory cells $M(\vec{y}, t)$, and effector cells $E(\vec{y}, t)$. The lifespan of a naive cell is of the order of a couple months. Memory cells, like naive cells can be stimulated in the same way to proliferate into effector cells and more memory cells. Memory cells live for decades. The effector cells are short-lived and do the work of removing the antigen from the system.

The stimulation rate of memory cells and naive cells, $\alpha H(\vec{x})\gamma(\vec{x}, \vec{y})$, is proportional to the cells affinity $\gamma(\vec{x}, \vec{y})$ for the presented antigen $H(\vec{x})$. The fraction of daughter cells from lymphocyte stimulation that become effector cells is f and the fraction that become memory cells is $1 - f$. The rate of antigen removal by effector cells is proportional to their affinity for the antigen, to the amount of antigen, and to the number of effector cells of that type.

Equations 2-5 can be solved analytically:

$$N(\vec{y}, t) = N(\vec{y}, 0)e^{-\alpha H(\vec{x})\gamma(\vec{x}, \vec{y})t}, \quad (6)$$

$$M(\vec{y}, t) = [M(\vec{y}, 0) + N(\vec{y}, 0)]e^{(1-2f)\alpha H(\vec{x})\gamma(\vec{x}, \vec{y})t} - N(\vec{y}, 0)e^{-\alpha H(\vec{x})\gamma(\vec{x}, \vec{y})t}, \quad (7)$$

$$E(\vec{y}, t) = \frac{2f\alpha H(\vec{x})\gamma(\vec{x}, \vec{y})}{(1-2f)\alpha H(\vec{x})\gamma(\vec{x}, \vec{y}) + \delta} [N(\vec{y}, 0) + M(\vec{y}, 0)] [e^{(1-2f)\alpha H(\vec{x})\gamma(\vec{x}, \vec{y})t} - e^{-\delta t}]; \quad (8)$$

$$A(\vec{x}, t) = A(\vec{x}, 0)e^{\beta t - \int d\vec{y} \int E(\vec{y}, t)\gamma(\vec{y}, \vec{x})dt}. \quad (9)$$

These solutions are only valid during the immune response. We consider these solutions up until the antigen level is reduced to half its initial value.

The simulations in this paper were performed with a two dimensional shape space on a 96×96 lattice. Table II gives the values of the model parameters used in the simulations. The parameters δ and $A(\vec{x}, t)$ were chosen to directly correspond with observed values. The other seven parameters were chosen to have approximate correspondence with seven related quantities such as the term of infection, the specificity of antigen-receptor binding, the total number of naive cells in an immune system, and the division time of the highest affinity lymphocytes. The seven equations used to estimate these model parameters are presented in the Supporting information along with the physiological values of the seven input parameters.

B. Primary Infection

To understand the basic behavior of the model for a single infection focus on the solid black set of curves in Fig. 2. The solid black lines in the four figures are the response to the first infection where the initial conditions are a uniform field of naive cells and no memory cells, Fig. 3 (left). In Fig. 2A we see the antigen response curve, $A(\vec{x}, t)$. In the absence of effector cells the antigen growth is exponential. The initial growth of antigen in the model is approximately exponential, but turns over as the effector cell population increases.

Figure 2B shows the total number of effector cells $E_T(t)$:

$$E_T(t) = \int E(\vec{y}, t)d\vec{y}, \quad (10)$$

Where the integral is over the entire shape space. The effector cell population size is initially equal to zero. After the antigen is removed the effector population decays exponentially back to zero with rate δ (not shown in Fig. 2).

Parameter	Value
$N(\vec{y}, 0)$	0.3 cells per lattice site
$A(\vec{x}, 0)$	10^5 cells
b	4 lattice sites
β	1.9 day^{-1}
αH	255 cells
γ_m	$0.01 \text{ cell}^{-1} \text{ day}^{-1}$
δ	0.01 day^{-1}
f	0.397
r_n	13.9 lattice sites

TABLE II: Values of parameters used in model simulations. Note that the product αH is listed rather than listing the parameters individually. Only the product arises in this model. H is the number of sites occupied by antigen during an immune response and α is a factor accounting for the difference in rates for the two affinity dependent processes: stimulation and antigen removal. The qualitative behavior of the model is not especially sensitive to precise parameter values.

As a measure of the quality of an immune response we introduce the Effectivity- $\Omega(t)$:

$$\Omega(t) = \int \gamma(\vec{x}, \vec{y}) E(\vec{y}, t) d\vec{y}. \quad (11)$$

The solid black line in Fig. 2C is a plot of $\Omega(t)$ for the primary infection. When $\Omega(t) = \beta$ the antigen curve turns over. Here β is plotted with $\Omega(t)$ for reference.

Figure 2D shows the average affinity $\bar{\gamma}(t)$:

$$\bar{\gamma}(t) = \frac{1}{E_T} \int \gamma(\vec{x}, \vec{y}) E(\vec{y}, t) d\vec{y}. \quad (12)$$

This quantity increases towards the maximum value of γ_m during the immune response as the highest affinity memory cells are re-stimulated most quickly; γ_m is plotted for reference. The rise in $\bar{\gamma}(t)$ is termed affinity maturation and in this model is solely due to affinity selection. Somatic-hypermutation, the rapid mutation of antibody genes, which is not considered in this model, provides an additional mechanism for more rapid convergence to γ_m . When the immune response has cleared the antigen from the system, long-lived memory cells are left behind.

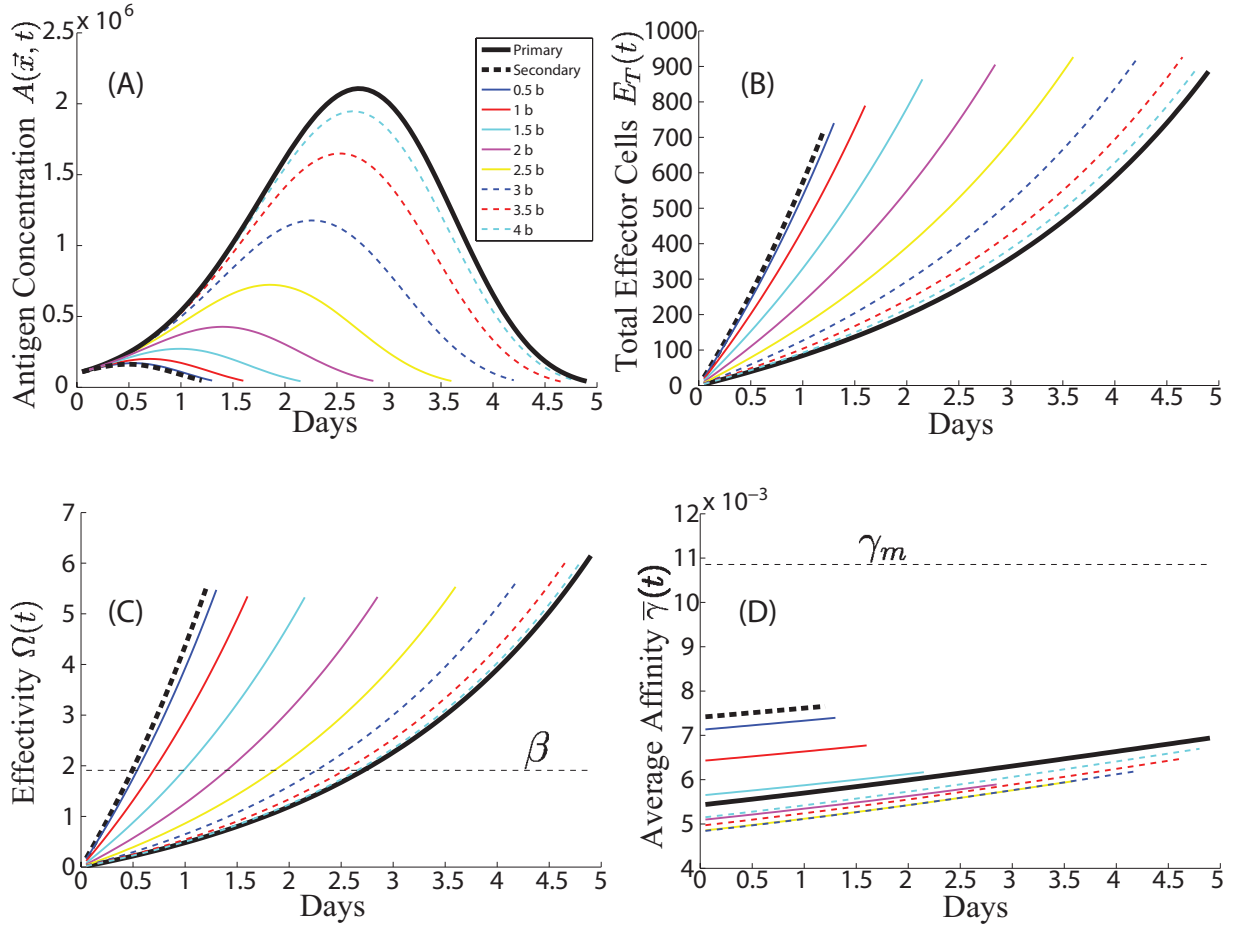


FIG. 2: These four figures show typical behavior of the model. The solid black curves show the response for the initial exposure, while the dashed black curves show the response to a second exposure of the same antigen. The colored curves show the response curves to related diseases following the initial exposure, with their colors corresponding to the markers in shape space drawn in 3. **A.** The $A(\vec{x}, t)$ curves. **B.** The total number of effector cells $E_T(t)$. **C.** The Effectivity- $\Omega(t)$ with β drawn for comparison. When the Effectivity is equal to β the $A(\vec{x}, t)$ curve turns over. **D.** The average affinity $\bar{\gamma}(t)$ with γ_m drawn for comparison. The $\bar{\gamma}(t)$ curve slowly and asymptotically approaches γ_m .

Figure 3 shows a small fraction of the shape space distribution of naive and memory cells before and after the immune response. Before the infection the distribution of lymphocytes is a uniform low level (all blue) field consisting only of naive cells. After the immune response there is an accumulation of memory cells that will survive indefinitely. This peak is centered on the antigen vector of the primary infection as naive and memory cells with receptor

vectors close to that proliferate most rapidly.

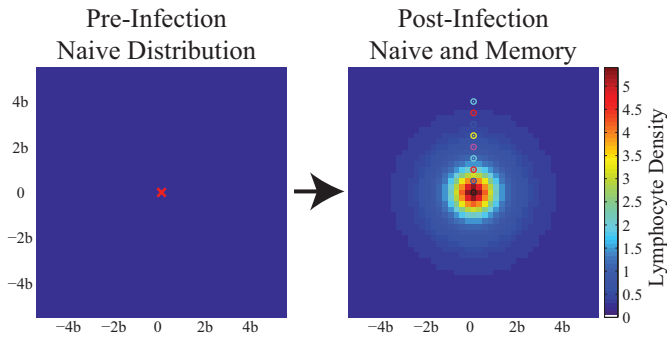


FIG. 3: The density of naive and memory lymphocytes in the shape space before and after an infection. The vector \vec{x} for the primary infection is shown as a red x in the center of the left figure. Initially the distribution is uniform consisting of only naive cells. After the immune response memory cells survive indefinitely. The memory cells are peaked around the antigen vector as the closest naive and memory cells have the highest proliferation rate, Eq. 1. The colored circles mark the locations of secondary infections studied in Section IID. The colors of the markers correspond to the colors of the plots in Fig. 2. Only a small portion of the total shape space, in the neighborhood of the primary infection, is shown. The shape space distance is measured in units of b which sets the scale in Eq. 1.

C. Immunity

In this section we consider the effect of memory cells in the generation of immunity to a disease. When the system is re-inoculated with the exact same antigen (center of Fig. 3), the memory cells provide an enhanced response. In Fig. 2 the black dashed lines show the response to a homologous secondary infection, where the initial memory and naive cell populations are shown in the right hand image in Fig. 3. The antigen pulse in Fig. 2A is shorter and lower in magnitude, a less severe disease for a shorter period of time. This is due to the much faster effector cell response shown in Fig. 2B and C. Again in 2C we see that when $\Omega(t) = \beta$ the antigen curve stops growing.

It should be noted that our model has no difference in the short term dynamics of memory cells and naive cells. The more rapid rise in effectors in Fig. 2B is due to the larger initial number of high affinity memory cells rather than an intrinsic difference in stimulation rate

for memory cells versus naive cells. The larger initial number of high affinity memory cells also gives rise to the increased average affinity of the secondary immune response seen in Figure 2D.

To quantify the severity of an infection we use the loss measure defined in [8]. This quantity is the integral over the $A(\vec{x}, t)$ pulse:

$$Loss = \int_0^{\infty} A(\vec{x}, t) dt. \quad (13)$$

The Loss is proportional to the resources the pathogen consumes, and the total amount of toxin the pathogen secretes over the course of the infection. For the primary and secondary infections in Fig. 2A, the loss was 4.9×10^6 and 1.5×10^5 respectively with units of Antigen \times days. The presence of memory cells at the start of the second infection reduced the severity of that infection.

D. Cross-Reactivity

We now turn our attention to secondary infections where the antigen differs slightly from the primary infection. The memory cells left from the primary infection can have some affinity for the heterologous secondary infection. This phenomenon is known as cross-reactivity or polyspecificity [17]. Cross-reactivity of memory cells is typically beneficial, such as the historic practice of vaccinating against smallpox with inoculation of the virus that causes cowpox. (Memory cells can have a negative cross-reactive effect if the antigen from the primary infection bears similarity to the self-antigens of the body, thereby inducing autoimmune disease [18]. We do not consider autoimmune effects here.)

To study the effects of cross-reactivity in the shape space picture, the vectors for the antigens of the primary and secondary infections must be similar. Mathematically the distance between the two shape space vectors must be within several b , the term that sets the shape space scale from Eq. 1. We look in detail at eight possible heterologous secondary infections separated from the primary infection by distances varying from $0.5b$ to $4b$. The colored circles drawn on the memory and naive distribution of Fig. 3 show the locations of the secondary infections in the shape space.

The colored lines in Fig. 2 show the secondary responses obtained from the model to the heterologous infections. The colors correspond to the circles drawn on the memory and

naive distribution of Fig. 3. The antigen time series plots in Fig. 2A show that as the shape space position of the secondary antigen moves away from the primary antigen, the infection becomes more severe. The antigen pulses are progressively longer in time and with larger maxima until the secondary antigen is far enough away that the curve is equal to the curve for the primary infection.

The blue curve in Fig. 4A shows the loss as a function of antigen position for the secondary infection. This curve asymptotically and monotonically approaches the loss of the initial infection as the secondary antigen moves away from the primary antigen in shape space. In the limit of zero antigenic difference we see the result discussed in Section II C for a homologous secondary infection. Cross-reactivity provides some immunity to diseases closely related to ones we have previously encountered.

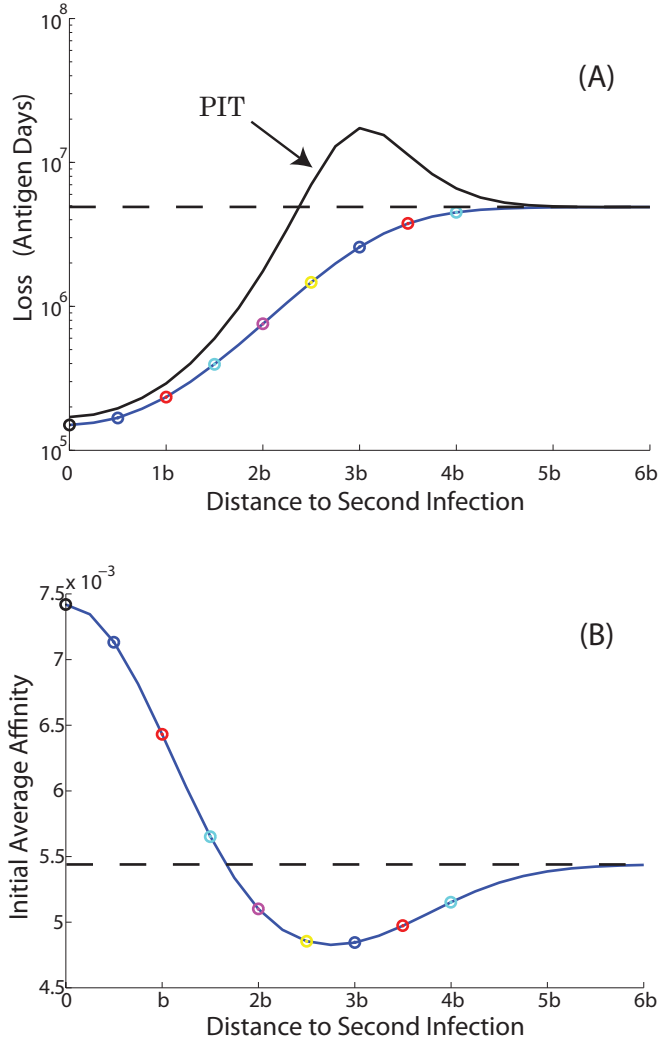


FIG. 4: **A.** The loss for secondary infections as a function of shape space distance from the primary infection to the secondary infection. First the blue curve illustrates the losses on the naive and memory distribution in the right hand image of Fig. 3. The blue curve shows the loss monotonically converging to the value for the primary infection as the distance increases. Now view the black curve for the negatively selected naive and memory cell distribution shown in the right hand image of Fig. 6. Both curves show the loss converging to the value of the primary infection as the antigenic distance increases. PIT is seen on the black curve when the loss for a secondary infection exceeds the loss for a primary infection. **B.** The initial average affinity, $\bar{\gamma}(0)$ for secondary infections as a function of shape space distance from the first antigen to the second. The dashed line illustrates $\bar{\gamma}(0)$ for a primary infection. As the distance increases $\bar{\gamma}(0)$ approaches the value for the primary infection. For distances greater than $1.75b$, $\bar{\gamma}(0)$ is less than the value for the primary infection. The colored circles on these plots correspond to the markers in Fig. 3 and Fig. 6 .

1. *Original Antigenic Sin*

In this subsection we describe the phenomena of “Original Antigenic Sin”. In Fig. 2D the average affinity curves, $\bar{\gamma}(t)$, for the heterologous responses show that moving away from the primary infection in shape space reduces the average affinity. This effect arises because the peak from the primary infection skews the distribution away from the uniform naive distribution. The average effector affinity can actually be lower than it would have been if there had not been a primary infection. This effect is more obvious in Fig. 4B, where we have plotted $\bar{\gamma}(0)$, the initial values of the average effector affinity as a function of the distance from the primary to secondary antigen. For a shape space distance greater than about $1.75b$, $\bar{\gamma}(0)$ is lower than for an unrelated infection.

This tendency for the adaptive immune system to respond with effectors specific to the primary infection in a heterologous immune response is known as “Original Antigenic Sin” [11]. This effect has been previously studied with more detailed and sophisticated models including somatic hypermutation [10]. While $\bar{\gamma}(t)$ is lower than it would have been for a primary response, as shown in Fig. 4B, $A(\vec{x}, t)$ is still lower in magnitude and shorter in time. The heterologous response in this scenario still has high affinity naive cells to use in its response; the presence of a large number of low affinity effector cells provides additional protection above what was available for a primary response. A measure of immune response quality that takes this into account is the Effectivity $\Omega(t)$ (Eq. 11), which is a measure of not only average affinity, but number as well.

The best example of the contrast between average affinity and effectivity in predicting infection severity, is given by the yellow curves in Fig. 2 which correspond to a shape space difference of $2.5b$ between the primary and secondary infections. The average affinity for the $2.5b$ infection is among the lowest studied, lower than the primary infection. The $A(\vec{x}, t)$ curve however shows only a moderate infection, much less severe than the primary infection. The rapid rise in the effectivity for the $2.5b$ infection better corresponds to this short term, low magnitude infection.

E. Pathogen Induced Tolerance

In this section we introduce Pathogen Induced Tolerance (PIT), a mechanism that can lead to a more severe secondary infection. Thus far our model has shown that memory cells, produced in response to an infection, can only have either a positive effect or no effect at all on future infections. How then might a primary infection create a vulnerability to some future infections? Immune system tolerance mechanisms inhibit the immune system from generating immune responses to self-antigens and harmless prevalent environmental antigens. When the immune system is tolerant to a pathogen the system ignores it leading to a more severe form of the disease. Here we show that inclusion of immune system tolerance in the model provides a mechanism by which a primary infection can leave the repertoire in a state vulnerable to heterologous infection.

1. Negative Selection

To describe PIT we include negative selection in our model. Negative selection describes the tolerance mechanism which eliminates autoreactive pre-naive cells before they mature. Pre-naive cells maturing in the bone marrow for B-cells, and in the thymus for T-cells, are presented antigen by dendritic cells. If the receptors of the immature lymphocytes bind to the presented antigen the resulting stimulation triggers the lymphocyte to die by apoptosis rather than proliferate as with naive cells. This is shown pictorially on the right hand side of Fig. 1. As many as 90% of the pre-naive cells are removed in this manner [13].

We model negative selection in the shape space as a perfect process removing all immature lymphocytes within a radius r_n . Figure 5 shows this effect on the distribution of naive cells. The pre-naive cells are derived from stem cells in the bone marrow, uniformly populating the shape space with their random receptors shown pictorially on the left. An antigen presented during negative selection is shown as a red x at the center of this distribution. The right hand image shows the naive cells that have matured. This distribution has a hole with radius r_n around the presented antigen where pre-naive cells were prevented from maturing.

The radius of cells that are positively selected r_p , must be smaller than r_n :

$$r_p < r_n. \tag{14}$$

If this were not the case, cells on the edge of the hole generated by negative selection would be

positively selected by self-antigens once mature. This would generate an immune response against those antigens, thereby generating autoimmune disease. Insuring that $r_p < r_n$ prevents the maturation of autoreactive lymphocytes and autoimmune disease.

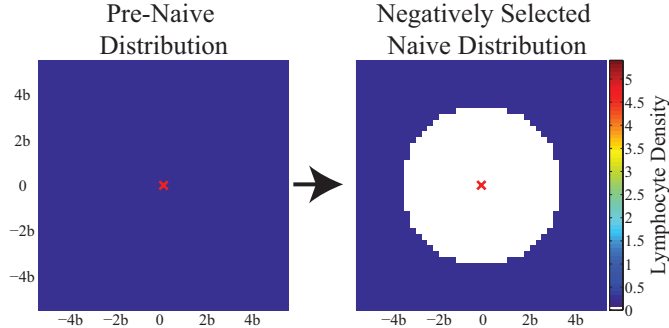


FIG. 5: Before and after negative selection: The left hand image shows the source of pre-naive cells. This is a uniform distribution. The shape space vector of antigen presented during negative selection is shown with the red x. The population of naive cells that emerge after surviving negative selection is shown at right. We have modeled this process as being perfect, eliminating all cells within radius r_n that are likely to be positively selected by that antigen were it encountered in the body.

Next we consider an infectious disease whose antigens are presented to not only naive and memory cells, but to pre-naive cells as well. Figure 6 shows the naive and memory cell population development for an infection that is incorporated into negative selection. This may happen from an infectious disease that persists for long periods in the body, such a virus with a long latent phase or a chronic bacterial infection.

The antigens from the persistent infection can be captured by dendritic cells and not only be presented in the lymph nodes to stimulate a response, but also to the pre-naive cells. The two left images in Fig. 6 repeat the reactions in Fig. 3. The middle distribution in this case is short-lived. As the naive cell population is turned over the replacement naive repertoire has a hole centered on the antigen from the infection.

The naive turnover takes place over a period of several months, thus the antigen from the primary infection must be presented in negative selection for at least this long in order for the hole to form. The right image shows the memory cells accumulated during the immune response in the center, with a naive cell distribution having a hole centered on the antigen from the primary infection giving the ring surrounding the memory cells.

A heterologous infection with antigen in the region where there are no memory cells and no naive cells in the right hand image of Fig. 6 will cause severe disease as the system is now unable to produce any high affinity effector cells. The immune system has become more tolerant to a subset of secondary infections due to the primary infection. This will lead to more severe disease from that subset of infections.

The loss as a function of the shape space distance between the primary and secondary infections is plotted in black in Fig. 4A. As can be seen in the figure, for parameters used in this paper, the loss exceeds the primary loss by as much as four times for serotypes with shape space distance greater than $2.25b$. This behavior is summarized in Table III. Note from Table III that this dynamic is symmetric. Primary inoculation with A or B induces tolerance and hence vulnerability to B or A respectively.

The loss as a function of shape space distance immediately following the primary infection is given by the blue curve in Fig. 4A. In the case of PIT this blue curve is short-lived and develops into the black curve over a period of several months as the naive cell population is turned over and the repertoire progresses from the middle image of Fig. 6 to the right hand figure. Observation of PIT relies on the antigen from the primary infection being presented over the several month naive recycling period in great enough quantity to produce the hole.

2. *Viral Latent Phase*

The lasting effects of pathogen induced tolerance (PIT) could vary widely. For an antigen that is unable to grow, such as a biologically inactive vaccine, or an antigen whose associated pathogen has been completely removed from the body, the PIT phase will be short-lived. The remaining antigen may degrade before the naive turnover is complete and the PIT vulnerability may never develop in this case. However, many viruses continue to live in the body, asymptotically, at low levels indefinitely after the immune response [19, 20]. This is known as the asymptomatic or latent phase of the infection. If a virus is living in the body at low levels its antigens should be active in negative selection. Viruses that create pathogen induced tolerance are not able to exploit this mechanism due to the presence of memory cells specific for them, Fig. 6 (right). The memory cells still give immunity to secondary homologous infections.

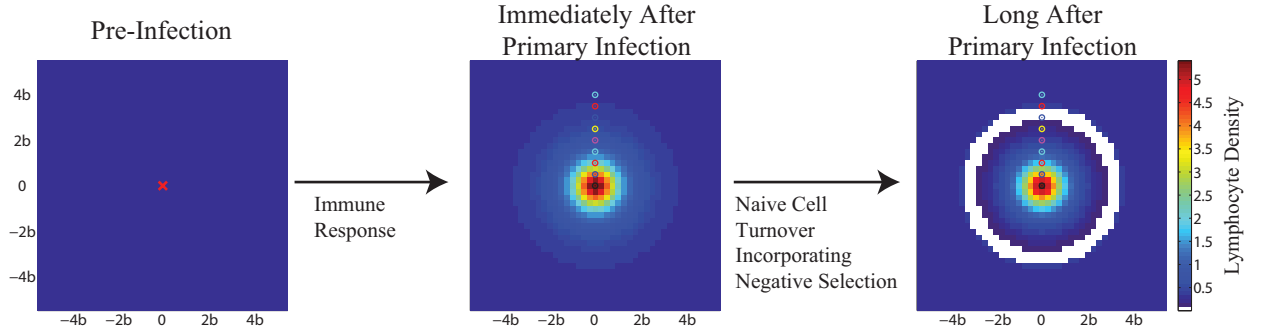


FIG. 6: The development of vulnerability after an infection whose antigen is incorporated into negative selection. The initial response to the primary infection is shown in the first two images. When the antigen participates in negative selection over the time scale of naive turnover, the lymphocyte density shown in the middle image will progress to the image at right. As the naive population is turned over, the replacement naive cells have a hole around the antigen from the first infection. The radius of the hole r_n must be larger than the radius of positively selected cells in order for negative selection to aid in prevention of autoimmune disease.

Primary Antigen	Primary Infection		Secondary Infection			
			Before Naive Turnover		After Naive Turnover	
	A_a	A_b	A_a	A_b	A_a	A_b
A_a	-		+	+	+	- -
A_b		-	+	+	- -	+

TABLE III: Phenomena predicted by model. A_a and A_b separated by a distance of around $3b$ in shape space. Normal infection and response (-), Immunity (+), Severe infection (- -)

III. DISCUSSION

The quality of the immune system response to an infection is a function of past exposures. A response to an antigen generates long-lived memory cells that are highly specific for that antigen. The memory cells confer immunity for future identical exposures, rapidly producing high affinity effector cells. A later exposure with a closely related antigen can also stimulate those memory cells but the effector cells produced will have a lower affinity for the new antigen. The presence of low affinity effector cells alone does not produce vulnerability, and average effector affinity is not necessarily a good measure of the quality of an immune

response. A better measure of the quality of an immune response, the effectivity, takes into account both affinity and total number of effectors. An infection can leave the system in a state vulnerable to a subset of related infections when the antigens of the initial infection are incorporated into the immune systems tolerance mechanisms, Pathogen Induced Tolerance.

Pathogen Induced Tolerance creates a state of vulnerability for the immune system. The signature of this mechanism is a short period of a few months with some degree of cross-reactive protection followed by a period of vulnerability. With a viral infection the vulnerability can last indefinitely via the latent phase of the virus. The PIT mechanism could be active for a number of disease systems. We consider below the dengue virus which has the signature behavior of PIT, and contrast PIT with other mechanisms proposed to explain the observed dengue phenomena.

A. Dengue

One disease system whose dynamics appear to be a strong candidate for the Pathogen Induced Tolerance mechanism is dengue. There are four closely related dengue virus serotypes. Infection with one serotype generates dengue fever and immunity to subsequent homologous infections. For a period of a few months [6, 21] there is also an observed beneficial immunity to heterologous infection with the other dengue serotypes. As predicted by our model this beneficial effect is observed to be short-lived and the system is observed to subsequently evolve to a state where infection with another serotype can progress to a more severe Dengue Hemorrhagic Fever (DHF) [6, 12].

An additional factor that suggests dengue may be an example of Pathogen Induced Tolerance involves a specific candidate pathway for the primary infection to participate in negative selection. Dendritic cells are highly permissive to the dengue virus. Dendritic cells are also the cells that present self-antigen during negative selection. This enhances the likelihood of dengue antigens taking place in negative selection during the asymptomatic phase of the infection. Furthermore, the time for naive cells to be recycled is of the same order as the cross-reactive benefit left from a primary infection with dengue [6, 21].

B. Original Antigenic Sin and Antibody Dependent Enhancement

Heterologous immune responses typically result in reduced severity. The more closely related two diseases are the more effective the memory cells from the primary infection will be when it comes to fighting the secondary infection. In cases where the heterologous secondary infection is more severe than it would have been if there were no primary infection, our model predicts that the effect can not be due to Original Antigenic Sin alone.

It has previously been suggested that Original Antigenic Sin itself generates the fragility to heterologous infections [10]. An alternate to PIT, which relies on Original Antigenic Sin has been proposed, and is referred to as Antibody Dependent Enhancement (ADE) [22]. In ADE low affinity antibodies facilitate the uptake of active virus into cells but do not inactivate the virus, thereby accelerating the infection of cells by virus.

However, ADE is incompatible with observed phenomena for dengue as ADE fails to capture the observed short term cross-reactive benefit from the primary dengue infection. This benefit lasts only months, but the ADE mechanism would be active from the onset of antibody production, preventing any transient benefit.

The PIT mechanism predictions match the observation of a period of short-lived beneficial cross-reactivity. In PIT the dengue antigens take part in negative selection and the mechanism predicts a short-lived beneficial cross-reactive effect that decays to vulnerability over months as the naive cells are recycled. The plausibility of this mechanism is aided by the observation that the dendritic cells that present self-antigen to the pre-lymphocytes are highly permissive to the Dengue virus. Dendritic cells infected by dengue, with virus in the latent phase, would be presenting dengue antigen in negative selection reactions. By this mechanism, our model and parameter estimates predict up to a factor of four increase in severity for the heterologous infection. This increase in severity could plausibly be the mechanism underlying the distinction between dengue fever (the primary infection) and the much more severe dengue hemorrhagic fever (the heterologous secondary infection). In the PIT mechanism the distinction is due to the lack of naive cells rather than presence of low affinity memory cells as predicted by ADE.

IV. ACKNOWLEDGEMENTS

This work was supported by the David and Lucile Packard Foundation and the Institute for Collaborative Biotechnologies through grant DAAD19-03-D-0004 from the U.S. Army Research Office.

SUPPORTING INFORMATION

Here we present equations for estimating seven of the model parameters given in table II. These equations are derived from seven related quantities which can be approximated from the model equations. Those approximations are then inverted to solve for the model parameters:

$$N(\vec{y}, 0) = \frac{N_t F}{l^d}; \quad (15)$$

$$r_n = \left[\frac{pN_t}{N(\vec{y}, 0)} \frac{\Gamma(d/2 + 1)}{\pi^{d/2}} \right]^{1/d}; \quad (16)$$

$$b = r_n \frac{1}{\sqrt{2 \ln\left(\frac{EDT}{MDT}\right)}}; \quad (17)$$

$$\beta = \frac{2}{t_e} \ln\left(\frac{A_m}{A(\vec{x}, 0)}\right) \left[1 + \sqrt{1 + \frac{\ln(2)}{\ln\left(\frac{A_m}{A(\vec{x}, 0)}\right)}} \right]; \quad (18)$$

$$f = \frac{1}{2} - \frac{MDT}{\ln(4)t_e} \ln\left(\frac{\Delta mem [2 \ln\left(\frac{EDT}{MDT}\right)]^{d/2}}{pN_t}\right); \quad (19)$$

$$\gamma_{max} = \frac{MDT \beta^2 [2 \ln\left(\frac{EDT}{MDT}\right)]^{d/2}}{4f \ln(2) pN_t \Gamma(d/2 + 1) \ln\left(\frac{A_m}{A(\vec{x}, 0)}\right)}; \quad (20)$$

$$\alpha H = \frac{\ln(2)}{MDT \gamma_{max}}. \quad (21)$$

The input parameters are:

- p , The specificity of the adaptive immune system is the probability that a randomly chosen lymphocyte and antigen bind strongly enough to stimulate the lymphocyte. We set p equal to 10^{-5} [23].
- N_t , the total number of naive lymphocytes. We set N_t equal to 2×10^7 , which is the value for a mouse [24]. This value will be higher in a human making the PIT effect more severe.

- MDT , the doubling time for the highest affinity lymphocytes. We set MDT equal to 6 hours, a standard estimate [1].
- EDT , the doubling time for the highest affinity self reactive lymphocytes, the lymphocytes on the edge of the sphere of negative selection. This must be at least as large as the naive cell lifetime. Incorporating T-help might relax this condition. We used EDT equal to 15 weeks.
- t_e , the length of time it takes to clear an infection. We used t_e equal to 10 days.
- A_m , the highest concentration of antigen during the primary infection. We set A_m equal to 10^7 [25].
- Δmem , the accumulated memory cells from a primary infection. We used Δmem equals 5000. The approximation for Δmem is order of magnitude.

The parameters MDT , EDT , t_e , A_m , and Δmem are approximated from the model using a Gaussian approximation for the $A(\vec{x}, t)$ pulse. The approximate equations (not shown here) for these parameters are then inverted to obtain the above equations. Additionally, the equations contain computational parameters d the dimension of the shape space, F the fraction of the total shape space we simulate, and l^d the number of lattice sites in the simulation. In this paper $d = 2$, $F = 8.1 \times 10^{-5}$, and $l^d = 96 \times 96$. We expect the qualitative behavior of the model to not be sensitive to precise values.

-
- [1] Kindt TJ, Osborne BA, Goldsby RA (2006) Kuby Immunology. W. H. Freeman, 6 edition, 574 pp.
- [2] Perelson AS, Weisbuch G (1997) Immunology for physicists. Reviews of Modern Physics 69:1219. URL <http://link.aps.org/abstract/RMP/v69/p1219>. Copyright (C) 2008 The American Physical Society; Please report any problems to prola@aps.org.
- [3] Workshop TI, Perelson AS (1987) Theoretical Immunology: The Proceedings of the Theoretical Immunology Workshop, Held June 1987, Santa Fe, New Mexico, volume 1 of *Proceedings volume in the Santa Fe Institute studies in the sciences of complexity*. Redwood City, Calif: Addison-Wesley Pub. Co, 407 pp.

- [4] Workshop TI, Perelson AS (1987) Theoretical Immunology: The Proceedings of the Theoretical Immunology Workshop, Held June 1987, Santa Fe, New Mexico, volume 2 of *Proceedings volume in the Santa Fe Institute studies in the sciences of complexity*. Redwood City, Calif: Addison-Wesley Pub. Co, 404 pp.
- [5] Vieira G, Chies J (2005) Immunodominant viral peptides as determinants of cross-reactivity in the immune system - can we develop wide spectrum viral vaccines? *Medical Hypotheses* 65:873–879. doi:10.1016/j.mehy.2005.05.041. URL <http://www.sciencedirect.com/science/article/B6WN2-4GR342Y-2/1/8accc7b8d3a8687a70c4be9021951409>.
- [6] Rothman AL (2004) Dengue: defining protective versus pathologic immunity. *The Journal of clinical investigation* 113:946–51. PMID: 15057297.
- [7] Welsh RM, Fujinami RS (2007) Pathogenic epitopes, heterologous immunity and vaccine design. *Nature reviews Microbiology* 5:555–63. PMID: 17558423.
- [8] Stromberg SP, Carlson J (2006) Robustness and fragility in immunosenescence. *PLoS computational biology* 2:e160. PMID: 17121459.
- [9] Perelson AS, Oster GF (1979) Theoretical studies of clonal selection: minimal antibody repertoire size and reliability of self-non-self discrimination. *Journal of theoretical biology* 81:645–70. PMID: 94141.
- [10] Deem MW, Lee HY (2003) Sequence space localization in the immune system response to vaccination and disease. *Physical Review Letters* 91:068101. doi:10.1103/PhysRevLett.91.068101. URL <http://link.aps.org/abstract/PRL/v91/e068101>. Copyright (C) 2008 The American Physical Society; Please report any problems to prola@aps.org.
- [11] Francis T (1960) On the doctrine of original antigenic sin. *Proceedings of the American Philosophical Society* 104:572–578. URL <http://links.jstor.org/sici?sici=0003-049X%2819601215%29104%3A6%3C572%3A0TD00A%3E2.O.CO%3B2-K>.
- [12] Alvarez M, Rodriguez-Roche R, Bernardo L, Vazquez S, Morier L, et al. (2006) Dengue hemorrhagic fever caused by sequential dengue 1-3 virus infections over a long time interval: Havana epidemic, 2001-2002. *Am J Trop Med Hyg* 75:1113–1117. URL <http://www.ajtmh.org/cgi/content/abstract/75/6/1113>.
- [13] Rolink AG, Schaniel C, Andersson J, Melchers F (2001) Selection events operating at various stages in b cell development. *Current Opinion in Immunology* 13:202–207. doi: 10.1016/S0952-7915(00)00205-3. URL <http://www.sciencedirect.com/science/article/>

B6VS1-42DP0BC-G/2/02469bbbd3a9d003be3103281d844dc4.

- [14] Beltman JB, Mare AFM, Lynch JN, Miller MJ, de Boer RJ (2007) Lymph node topology dictates t cell migration behavior. *The Journal of experimental medicine* 204:771–80. PMID: 17389236.
- [15] Kemir C, Boer RJD (1999) A mathematical model on germinal center kinetics and termination. *Journal of immunology (Baltimore, Md : 1950)* 163:2463–9. PMID: 10452981.
- [16] Smith DJ, Forrest S, Hightower RR, Perelson AS (1997) Deriving shape space parameters from immunological data. *Journal of theoretical biology* 189:141–50. PMID: 9405131.
- [17] Wucherpfennig KW, Allen PM, Celada F, Cohen IR, Boer RD, et al. (2007) Polyspecificity of t cell and b cell receptor recognition. *Seminars in Immunology* 19:216–224. doi:10.1016/j.smim.2007.02.012. URL <http://www.sciencedirect.com/science/article/B6WX3-4NCKJXX-1/1/0408b7b7bc67d1c2dc162bcc2df6cb9f>.
- [18] Oldstone MB (2005) *Molecular Mimicry: Infection Inducing Autoimmune Disease*. Springer, 1 edition, 168 pp.
- [19] Nowak MA, May R (2001) *Virus dynamics: Mathematical principles of immunology and virology*. Oxford University Press, USA, 256 pp.
- [20] Enquist LW, Racaniello VR, Skalka AM, Flint SJ (2000) *Principles of Virology: Molecular Biology, Pathogenesis, and Control of Animal Viruses*. American Society Microbiology, 2 edition, 918 pp.
- [21] SABIN AB (1952) Research on dengue during world war ii. *The American journal of tropical medicine and hygiene* 1:30–50. PMID: 14903434.
- [22] Morens DM, Halstead SB (1990) Measurement of antibody-dependent infection enhancement of four dengue virus serotypes by monoclonal and polyclonal antibodies. *The Journal of general virology* 71 (Pt 12):2909–14. PMID: 2273390.
- [23] Klinman NR, Press JL (1975) The b cell specificity repertoire: its relationship to definable subpopulations. *Transplantation reviews* 24:41–83. PMID: 49962.
- [24] Khaled AR, Durum SK (2002) Lymphocyte: cytokines and the control of lymphoid homeostasis. *Nature reviews Immunology* 2:817–30. PMID: 12415306.
- [25] Thakar J, Piloni M, Kirimanjeswara G, Harvill ET, Albert R (2007) Modeling systems-level regulation of host immune responses. *PLoS computational biology* 3:e109. PMID: 17559300.